Computer Vision Winter Workshop 2007, Michael Grabner, Helmut Grabner (eds.)
St. Lambrecht, Austria, February 6–8
Graz Technical University

A Robust Model based Algorithm for Detection of Singularities in Fingerprint Images

Surinder Ram[1], Horst Bischof[1], and Josef Birchbauer[2]

[1]Technical University of Graz, Austria
{ram,bischof}@icg.tu-graz.ac.at
[2]Siemens PSE Austria
josef-alois.birchbauer@siemens.com

Abstract *The performance of fingerprint recognition is heavily depending on the reliable extraction of singularities. Common algorithms are based on a Poincáre-Index estimation which is a numerical method. These algorithms ignore the topology of the underlying data and are only robust when certain heuristics and rules are applied. In this paper we present a model based approach for the detection of singular points. The presented method exploits the geometric nature of linear differential equation systems. Our method is robust against noise in the input image and is able to detect singularities even if they are partly occluded. The algorithm proceeds by fitting parameters for a given patch and then analyses these parameters. The parameters give a measure for the significance of the underlying structure and the type of a possible singularity. Corollary, our algorithm also reconstructs the direction field near a singular point which greatly aids the extraction of minutiae in these regions.*

1 Introduction

Fingerprint matching is a very suitable method for identifying people. The application of fingerprint based personal authentication and identification is steeply increasing. The use of this technology can be seen in forensics, commercial industry and government agencies, to mention a few. Fingerprints are attractive for identification because they can characterize an individual uniquely and their configuration do not change through the life of individuals except of bruises, cuts or other alterations on the fingertips [**?**]. In general, personal verification or identification based on fingerprints mainly consists of acquisition, feature extraction, matching and a final decision.

1.1 The Role of Singularities in Fingerprint Matching

Fingerprints can be classified into five categories: arch, tented arch, left loop, right loop and whorl. The first step in an identification system is the classification of a given fingerprint [**?**]. This reduces the amount of data to be searched for matches as the database can be partitioned into subsets. Especially for large scale applications this results in a vital speed up. Common algorithms extract singular points in fingerprint images and perform classification based on the number and location of these singularities.
After this classification task, the fingerprints are matched against a given template in the database. For this purpose it is needed to extract minutiae, which are special points in fingerprints where ridges end or bifurcate. Two fingerprints can be reported as equal, if a certain number of minutiae positions are identical in the two fingerprints. In general, matching of fingerprint images is a difficult problem [**?**], mainly due to the large variability in different impressions of the same finger (i.e. displacement, rotation, distortion, noise, ...). One way to relax the problem in terms of performance and runtime is to use certain ”landmarks” in the image in order to apply a pose transformation. Since singular points are unique landmarks of fingerprints, commonly they are used as reference points for matching [**?**].

1.2 Methods for Extraction of Singularities in Fingerprintimages

There are many approaches proposed for singular point detection in literature. Karu and Jain [**?**] referred to a Poincáre-Index method. However, there are principal weaknesses adhered to the method. Many rules and heuristics have been proposed by different authors (e.g.[**?**]) in order to make the method robust against noise and minor occlusions. Due to it's simplicity and more than adequate performance in most images, this method enjoys high popularity in fingerprint recognition systems.

Another method, described in [**?**] exploits the fact that partioning the orientation image in regions characterized by homogeneous orientations implicitly reveals the position of singularities. The borderline between two adjacent regions is called a fault-line. By noting that fault lines converge towards loop singularities and diverge from deltas, the authors define a geometrical method for determining the convergence and divergence points.

Nilson et al. [**?**] identify singular points by their symmetry properties. In particular this is done using complex filters, which are applied to the orientation field in multiple resolution scales. The detection of possible singularities is done by analysing the response created by these complex filters.

1.3 Model based detection of Singularities

In [?] Rao et al. proposed a novel algorithm for singular point detection in flow fields. A window of fixed size is sweeped over the entire image. At each location of the window, the model parameters are fitted. Once these parameters are obtained at each point, operations like classifying the image and locating critical points can be done. Their application is mainly limited to the detection of saddles and spirals of flow field images. The authors also mentioned a possible application of the method to fingerprint images.

Fingerprint singularities have different properties than commonly found in flow fields, where mostly whorls and saddles appear. Another feature of flow fields is that the aspect ratio of the singularities is approximately one. Flow field singularities can be modeled by the authors method, while fingerprint singularities generally not. Even though, center and spiral shaped singularities are present in fingerprint images, loops and deltas need a completely new method for characterisation.

In this paper we present a novel method for the detection of singularities based on the work of Rao et al. In comparison, our method is robust against noise in the input image and is able to detect singularities even if they are partly occluded. Additionally, we present a method for detection and recognition of all types of singularities in fingerprint images. This model based attempt is new to the field of fingerprint singularity detection.

1.4 Outline

In section **??** an explanation of phase portraits is given. Furthermore the fitting of the parameters and algorithms are explained in detail. Moreover we analyse the weaknesses of the original algorithm and propose a robust method.

In section **??** we explain how this algorithm can be applied to fingerprint images.

Section **??** shows the conducted experiments. In the first part, we demonstrate the abilities of our robust method using synthetic data. Furthermore we show the application of the algorithm on several fingerprints with occlusions and noise.

In the last section a summary of the proposed method is given.

2 Two-Dimensional Linear Phase Portraits

Phase portraits are a powerful mathematical model for describing oriented textures, and therefore have been applied by many authors [?, ?, ?] in their work. Linear phase portraits can be expressed by the following differential equation system:

$$\frac{dx}{dt} = \dot{x} = p(x,y) = cx + dy + f \qquad (1)$$

$$\frac{dy}{dt} = \dot{y} = q(x,y) = ax + cy + e \qquad (2)$$

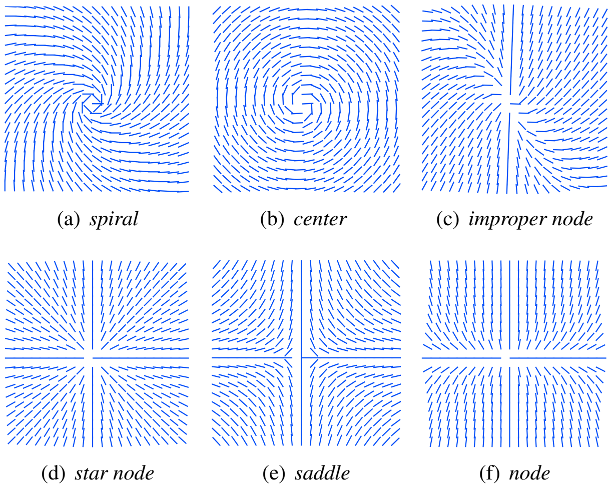
(a) *spiral* (b) *center* (c) *improper node*
(d) *star node* (e) *saddle* (f) *node*

Figure 1: A classification of different phase portraits based on the characteristic matrix $\vec{A}$ [?]. Complex eigenvalues result in **??** and **??**, differntiated from each other only by the real part of the eigenvalues. If the eigenvalues are real and both equal, the pattern can be classified into a startnode **??** or into an improper node **??**. Miscellaneous real valued eigenvalues result in a saddle **??** or a node **??**, depending on their signs. The saddle type differs from the node by having opposite signed eigenvalues.

By varying the parameter of these equations we can describe a set of oriented textures comprising saddles, star nodes, nodes, improper nodes, centers and spirals [?] (examples are given in figure **??**). The orientation of these fields can be given by:

$$\phi(x,y) = atan\left(\frac{dy}{dx}\right) \qquad (3)$$

$$\phi(x,y) = atan\left(\frac{\dot{y}}{\dot{x}}\right) = atan\left(\frac{ax+by+e}{cx+dy+f}\right) \qquad (4)$$

Equation **??** and **??** can further be represented in a more convenient matrix notation as:

$$\dot{\vec{X}} = \vec{A} * \vec{X} + \vec{B} \qquad (5)$$

where $\vec{X} = \begin{bmatrix} x \\ y \end{bmatrix}, \vec{A} = \begin{bmatrix} c & d \\ a & b \end{bmatrix}, \vec{B} = \begin{bmatrix} f \\ e \end{bmatrix},$

$\vec{A}$ is called the *characteristic matrix* of the system. A point at which $\dot{x}$ and $\dot{y}$ are zero is called a *critical point* (x_0, y_0) [?]. The elements of the characteristic matrix are used to determine six flow patterns.[?]. The type of the flow pattern is determined by the eigenvalues of the chararacteristic matrix.

2.1 Parameter extraction

Rao and Jain [?] presented an algorithm for the parameter extraction of oriented textures. The non-linear least squares computation required in their algorithm is computationally expensive and prone to local minima.

In [?] Shu et al. presented a linear formulation of an algorithm which computes the critical points and parameters for a two dimensional phase portrait. Because their approach is linear there exists a closed form solution.

In the following section we give a brief introduction of the algorithm presented by Shu et al. in [**?**, **?**]. To solve the problem we can apply a least squares algorithm. Eqation (**??**) can be expressed as:

$$p(x_i, y_i) - tan\phi_i * q(x_i, y_i) = 0 \tag{6}$$

We can directly estimate the parameters by using the triplet data $(x_i, y_i, tan\phi_i)$ and (**??**), where (x_i, y_i) is the coordinate of a pixel and the $tan\phi_i$ the observed data. Let $tan\phi_i = \zeta$; The optimal weighted least square estimator is one that minimizes the following cost function:

$$\sum_{i=0}^{n} \omega_i^2 \cdot [p(x_i, y_i) - \zeta_i \cdot q(x_i, y_i)]^2, \tag{7}$$

which can be rewritten as:

$$\sum_{i=0}^{n} \omega_i^2 \cdot [ax_i + by_i - \zeta_i cx_i - \zeta_i dy_i + e - \zeta_i f]^2 \tag{8}$$

and subject to the constraint:$\sqrt{a^2 + b^2 + c^2 + d^2} = 1$. Where $w_i = cos\phi_i$, and is used because the tangent function is not uniformly sensitive to noise, so each observed data has to be weighted by the inverse of the derivate of the tangens function. n is the total number of triplet data used to estimate the parameter set (a, b, c, d, e, f).

Let

$$L_4 = \begin{bmatrix} a \\ b \\ c \\ d \end{bmatrix}, L_2 = \begin{bmatrix} e \\ f \end{bmatrix}, \Omega_2 = \begin{bmatrix} \omega_0 & -\zeta_0\omega_0 \\ \omega_1 & -\zeta_1\omega_1 \\ \omega_2 & -\zeta_2\omega_2 \\ \vdots & \vdots \\ \omega_n & -\zeta_n\omega_n \end{bmatrix}$$

and

$$\Omega_4 = \begin{bmatrix} x_0\omega_0 & x_0\omega_0 & \zeta_0 x_0\omega_0 & \zeta_0 y_0\omega_0 \\ x_1\omega_1 & x_1\omega_1 & \zeta_1 x_1\omega_1 & \zeta_1 y_1\omega_1 \\ x_2\omega_2 & x_2\omega_2 & \zeta_2 x_2\omega_2 & \zeta_2 y_2\omega_2 \\ \vdots & \vdots & \vdots & \vdots \\ x_n\omega_n & x_n\omega_n & \zeta_n x_n\omega_n & \zeta_n y_n\omega_n \end{bmatrix}$$

Now we can express the previous constrained optimization as minimizing the cost function:

$$C = (\Omega_4 L_4 + \Omega_2 L_2)^T(\Omega_4 L_4 + \Omega_2 L_2) + \lambda(L_4^T L_4 - 1) \tag{9}$$

Differenciating C with respect to L_4, L_2 and to the langrangian multiplier λ, and setting the derivates to zero, we obtain:

$$\frac{\partial C}{\partial L_4} = 2\Omega_4^T\Omega_4 L_4 + 2\Omega_4^T\Omega_2 L_2 + 2\lambda L_4 = 0$$

$$\frac{\partial C}{\partial L_2} = 2\Omega_2^T\Omega_2 L_2 + \Omega_2^T\Omega_4 L_4 = 0$$

$$\frac{\partial C}{\partial \lambda} = L_4^T L4 - 1 = 0$$

which yields:

$$L_4^T L4 = 1$$

$$L_2 = -(\Omega_2^T\Omega_2)^{-1}\Omega_2^T\Omega_4 L_4 \tag{10}$$

$$\psi L_4 = \lambda L_4 \tag{11}$$

where:

$$\psi = -\Omega_4^T\Omega_4 + \Omega_4^T\Omega_2(\Omega_2^T\Omega_2)^{-}1(\Omega_2^T\Omega_4). \tag{12}$$

L_4 is an eigenvector of the symmetric matrix ψ and λ is its eigenvalue. Therefore, the eigenvector with the smallest absolute eigenvalue gives the best estimation of L_4. We can further compute L_2 by using Equation (**??**).

2.2 Algorithm Analysis

In [**?**] Shu et al. refined their algorithm and presented a detailed analysis for their algorithm. From this analysis and our own experiments two conclusions can be drawn:

1. The presented algorithm works well in the case of Gaussian distributed noise. In the presence of occlusions, the algorithm may fail to extract the correct parameters.

2. The method has non uniform sensitivity to noise - depending on the position of the point. The sensitivity in regions close to the singular point is low, whereas the sensitivity in regions away from the singular points is increased. The reason for this property of the algorithm is that not the ratio of the two functions $p(x, y)$ and $q(x, y)$ is optimized, but rather the difference (see equation **??**).

2.3 RANSAC based approach

Although the roots of the linear phase portrait estimation algorithm can be tracked back to the year 1990 [**?**], only recently several authors applied this algorithm in their work. For example in [**?**], the authors applied this algorithm in order to extract a high level description of fingerprint singularities and direction fields thereof. As mentioned above, there are conceptional weaknesses adhered to this algorithm. In order to improve the performance of the original algorithm we propose the following RANSAC [**?**] based approach:

1. Randomly select 6 triplet data points (x, y, ζ) from the oriented texture and compute the model parameters using the algorithm described above.

2. Verify the computed model by using a voting procedure. Every pixel lying within a user given threshold t, increases the vote.

3. If the vote is big enough, accept fit and exit with success.

4. Repeat 1-3 for n times

The number of iterations n can be computed using the following formula [**?**]:

$$n = \frac{log(1 - z)}{log[1 - (1 - \epsilon)^m]} \tag{13}$$

Where z is the confidence level, m is the number of parameters to be estimated and ϵ is the outlier proportion.

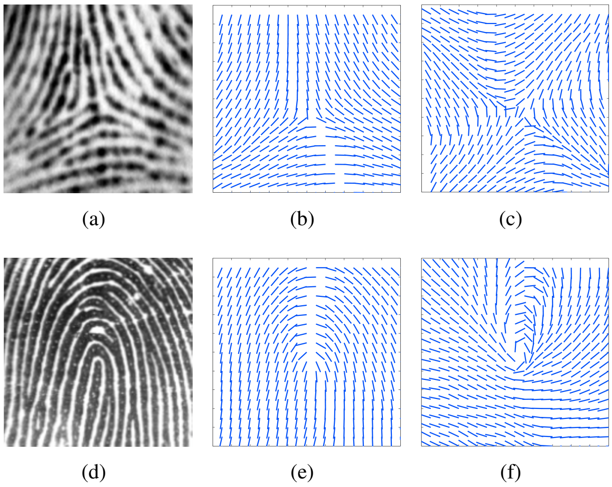

Figure 2: The orientation fields of a delta **??** and a loop **??** respectively. The doubled angle orientation fields can be seen in figure **??** and **??**. Note the non centric appearance of **??**. Thus the loop can not be modeled either in the original orientation field nor in the doubled angle orientation field. The delta can be modeld using the doubled angle orientation field as a saddle type singularity.

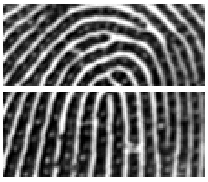

Figure 3: The proposed method for loop detection. First, a half circle (upper part) is detected. In a further step it is analysed if the half circle is surrounded by a homogeneous region.

Appearance	Eigenvalues	Thresholds
Whorl 	complex eigenvalues $\lambda_1 = \Re + j\Im$ $\lambda_2 = \Re - j\Im$	$\frac{1}{3} < \frac{\lambda_1}{\lambda_2} < 3$
Delta 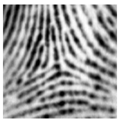	real distinct eigenvalues λ_1 and λ_2 with opposite sign	$\frac{1}{4} < \frac{\lambda_1}{\lambda_2} < 4$
Loop 	upper part only: complex eigenvalues $\lambda_1 = \Re + j\Im$ $\lambda_1 = \Re - j\Im$	$\frac{1}{3} < \frac{\lambda_1}{\lambda_2} < 3$ $\Re < 0.2$

Table 1: In this table the classification schema of the different singularities in fingerprint can be seen. In principle the classification is done based on the extracted parameters of the model. Whorls are detected in the original orientation field which is extracted gradient based. The detection of deltas is done in the doubled angle orientation field. In case of the loop, first a half center is detected, followed by the detection of a homogeneous region. The shown thresholds were introduced in order to prevent the fitting of physically impossible parameters.

3 Application to Fingerprint Singularities

In [**?**] the authors noted that the doubled angle orientation field of a delta shows the pattern of a saddle and a loop shows the pattern of a center (see figure **??**). The aim of the authors was to find constraints for the nonlinear phase portrait model they proposed in the paper. For the detection of fingerprint singularities the authors proposed a Poincáre Index based method. Although the authors successfully applied this methodology to selected images, their approach fails with most given loops in fingerprint images. The reason therefore lies in the non-centric appearance of the doubled angle field of the loop. Hence in general a loop can not be described using linear phase portraits. On the other hand the doubled orientation field of a delta can be very well applied practically.

3.1 A Model for Loop type Fingerprint Singularities

For loops in fingerprint images we propose a different method. First, we detect a half circle in the image, then in a further step the half circle is analysed for homogeneous regions. (See figure **??** for an example)

3.2 Parameter analysis

Once parameters for a given sub window are fitted, these parameters must be inspected for their meaning. This inspection is done using the eigenvalues of the characteristic matrix $\vec{A}$. In general the ratio of the two eigenvalues $\frac{\lambda_1}{\lambda_2}$ is expressing the aspect ratio of a oriented pattern around a given singularity. In order to prevent physically impossible parameters to be fitted, we introduced a threshold for this ratio.

If the eigenvalues are complex numbered, then the analysed window contains a whorl. If the eigenvalues are real valued and with opposite sign, then the analysed patch contains a delta. In table **??** an overview of the classification and the thresholds are given.

4 Experimental Results

4.1 Fitting on synthetic data

In the following, a small comparison between the original algorithm and the one proposed by us is given. The data used has been created synthetically using equation (**??**). In figure **??** a noise test is performed. Figure **??** shows how the both methods handle occlusions. While the original method fails extracting the correct model parameters, our approach is robust against these occlusions. In figure **??** we conducted a test in order to explain the non uniform sensitivity of the original algorithm. As can be seen from this experiment our algorithm is uniform sensitive.

4.2 Fitting on real Fingerprint Singularities

In this section we show the model fitting capability of the proposed method. Input images for the algorithm are taken from regions around singular points. The images contain a certain number of occlusions. The estimation of the

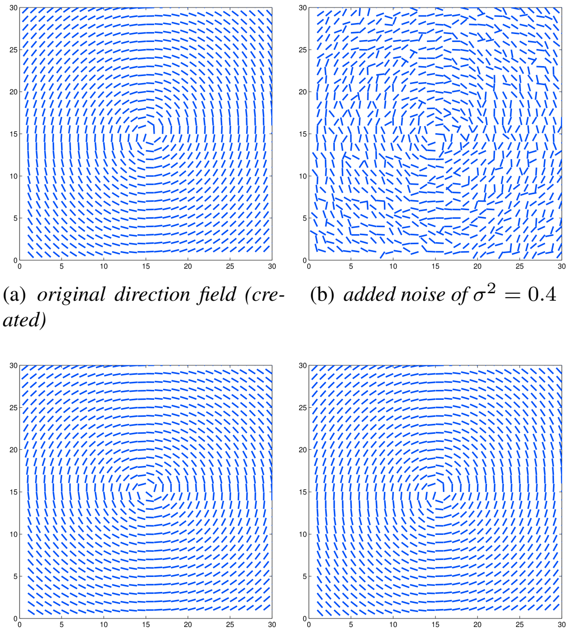

(a) *original direction field (created)* (b) *added noise of $\sigma^2 = 0.4$*

(c) *reconstructed using original Algorithm.* (d) *reconstructed using proposed algorithm.*

Figure 4: This test is similar to the test performed by Shu et al. [**?**] which was conducted in order to show the robustness of their algorithm. The generated pattern is of center type. Normal distributed noise with $\sigma^2 = 0.4$ has been added to the direction field. Both algorithms are almost immune to this type of contamination and are able to reconstruct the noisy direction field.

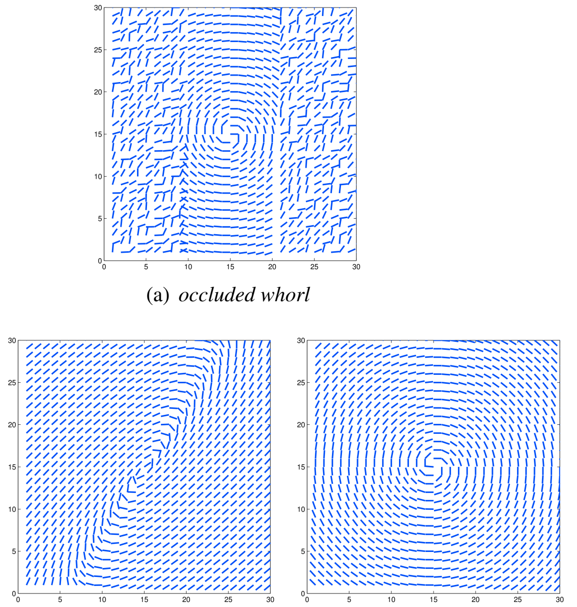

(a) *occluded whorl*

(b) *reconstructed by original method* (c) *reconstructed by proposed method*

Figure 5: In this example we compare the robustness of the two algorithms against occlusions. First an orientation field of center type has been created. On both sides of the orientation field a occlusion has been simulated by replacing the original values by random values. While the original algorithm fails (figure **??**), our new approach (figure **??**) extracts the parameters precisely.

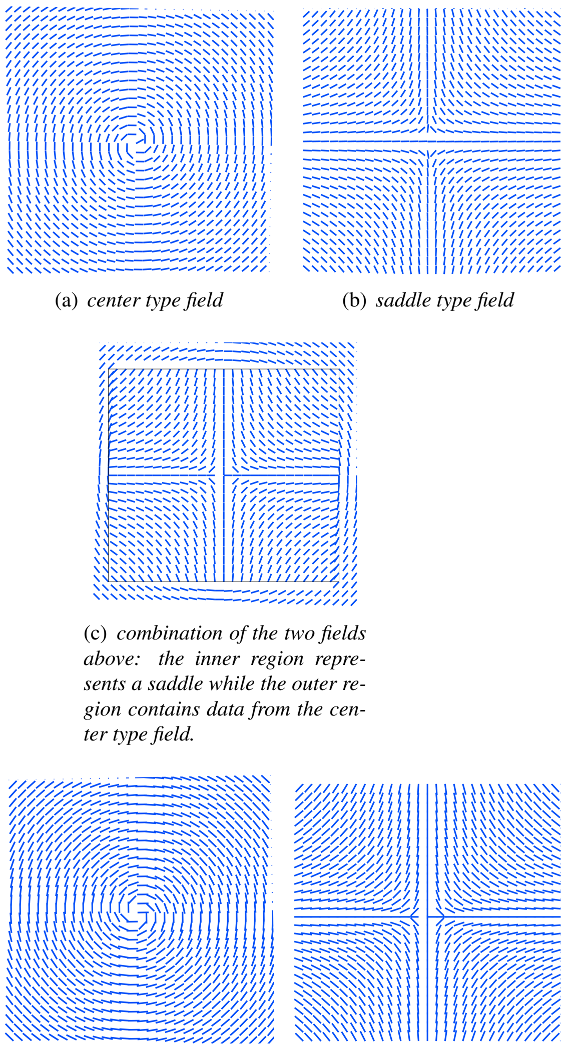

(a) *center type field* (b) *saddle type field*

(c) *combination of the two fields above: the inner region represents a saddle while the outer region contains data from the center type field.*

(d) *reconstructed using original Algorithm* (e) *reconstructed using proposed Algorithm*

Figure 6: This example demonstrates the non uniform sensitivity of the original algorithms. Figure **??** and **??** are used to construct the direction field shown in figure **??**. The original algorithm of Shu et al. [**?**] gives more emphasize to points which are away from the potential singular point. Although more than two thirds of the data correspond to a saddle type orientation field, the original algorithm **??** still reconstructs a center type field. Our method **??** on the other hand extracts the expected results.

orientation field is accomplished by the algorithm of Rao and Schunk [**?**].

In figure **??** a delta with many artificial occlusions can be seen. At the occlusions, the orientation data is not determined correctly. With aid of the proposed method, the correct model parameters can be obtained.

An example of a whorl type singularity with wrongly detected orientations can be seen in figure **??**. Our algorithm detects the correct model parameters and it is possible to refine the original orientation field in areas where it was wrongly extracted.

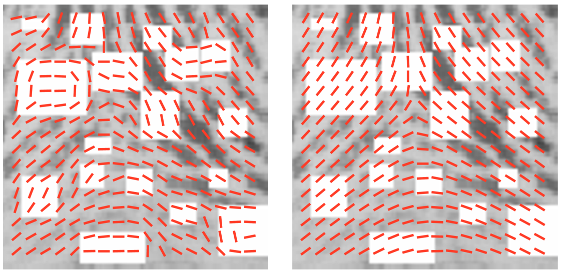

(a) *gradient based* (b) *refined through model*

Figure 7: Parameter fitting for a delta type singularity. The orientation field in figure **??** was generated by using a gradient based method [**?**]. Occlusions are regions where the gradients can not be correctly extracted. These regions (white colored) are artificial and have been added by hand. In figure **??** it is visualized how the proposed algorithm was capable of fitting the correct model parameters. Note that our method not only detects the singular point robustly, but also smooths the orientation field.

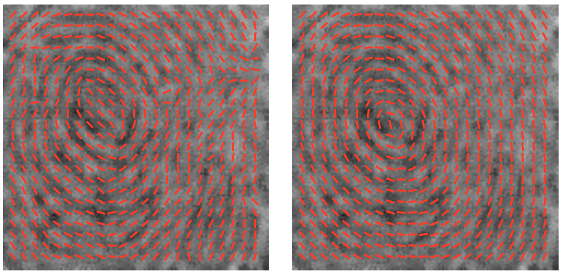

(a) *gradient based* (b) *refined through model*

Figure 8: Figure **??** shows a low quality fingerprint image with the orientation image extracted from gradients. In figure (**??**) the successful application of the proposed algorithm can be seen. The singularity and orientation field have been determined successfully.

The proposed method for the loop type singularties is shown in figure **??**.

Figure **??** shows the results on a spiral. Note how the proposed algorithm predicts the correct orientations where the gradient based method fails. What also can be seen is that directional filtering uncovers a lot of detail from the underlying data. But directional filtering can only be successfully applied when the correct orientation field is present.

4.3 Singular Point Detection in Fingerprint Images

In this subsection we present results of the detection and recognition algorithm. All shown images have been taken from the Fingerprint Verification Competition [**?**, **?**]. The position of the sliding window is marked with a rectangle.

In figure **??** the detection is performed on a loop type fingerprint image.

Figure **??** shows the detection results on a whorl type fingerprint.

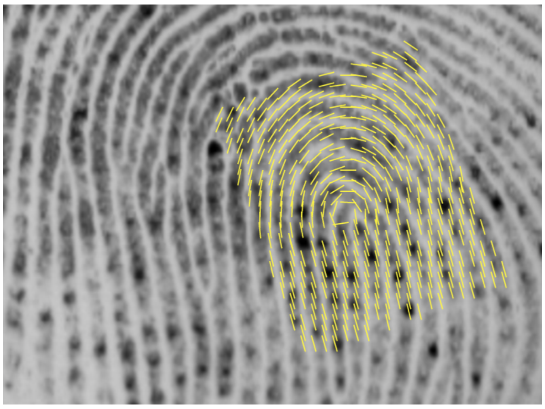

Figure 9: The proposed model fitted to a loop, the upper part as circle and the lower part as homogeneous area.

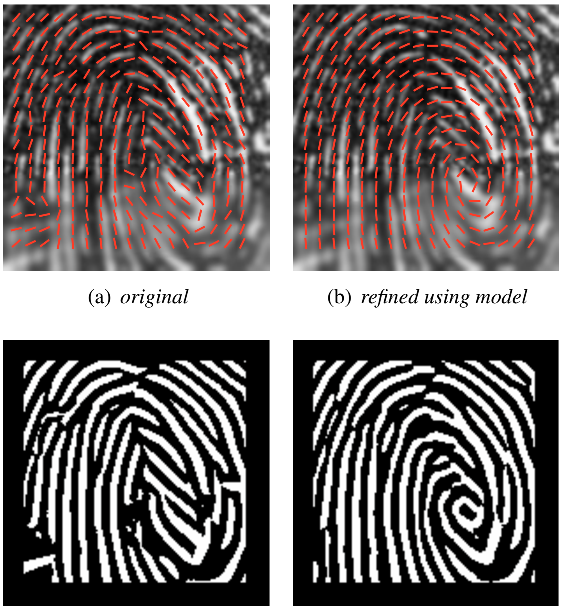

(a) *original* (b) *refined using model*

(c) *gabor filtered* **??** (d) *gabor filtered* **??**

Figure 10: A low quality image of a spiral type singularity. The gradient based extraction of the orientation field results in the shown orientation field in figure **??**. In figure **??** this orientation field has been refined using our approach. In figure **??** and **??** it is shown how directional filtering using Gabor filters can improve the clarity of ridges and furrows of such regions.

A slightly rotated whorl can be seen in figure **??**. The region around the delta is of bad quality.

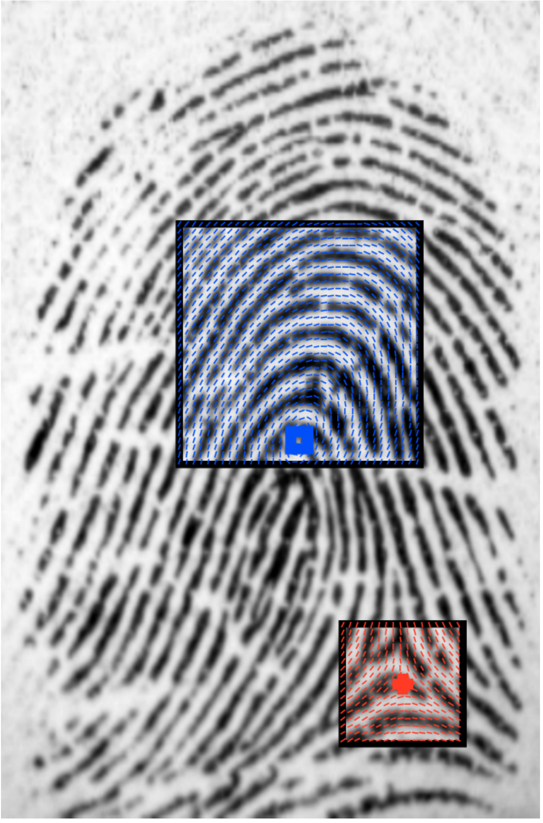

Figure 11: In this example the detection of singularities of a loop type fingerprint singularity can be seen.

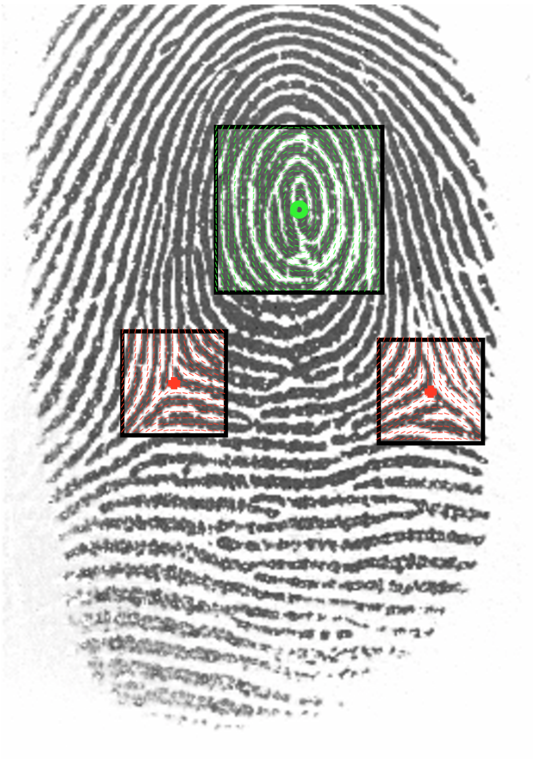

Figure 12: This example shows the detection of a whorl and two deltas.

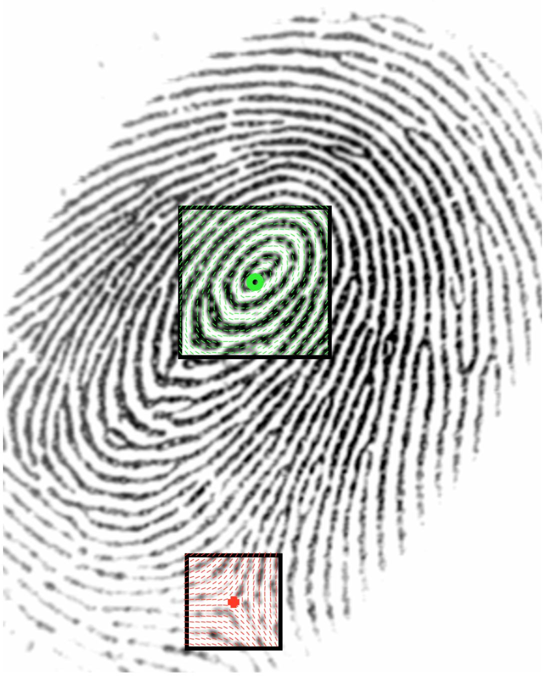

Figure 13: This figure shows the detected singularities in a whorl type fingerprint.

5 Conclusion

We presented a model based method for singular point detection in fingerprint images. Our proposed method is robust to noise and occlusions in the input image. The algorithm proceeds by fitting model parameters at each location of a sliding window and then analyses this model parameters. On positions of singular points, a detection can be performed by the analysis of these parameters.

We performed several tests on synthetic and natural images in order to show the mentioned capabilities of our algorithm. We also showed how the algorithm is able to reconstruct the orientations near singular points. In the last part of this paper we showed detection results of the proposed algorithm.

Future work includes the testing of our method with larger datasets. Furthermore we aim at merging our model based approach with existing numerical methods.

Acknowledgement

This work was funded by the Biometrics Center of Siemens PSE Graz.

References

[1] Martin A. Fischler and Robert C. Bolles. Random sample consensus: a paradigm for model fitting with applications to image analysis and automated cartography. *Commun. ACM*, 24(6):381–395, June 1981.

[2] R. M. Ford and R. N. Strickland. Nonlinear phase portrait models for oriented textures. *Computer Vision and Pattern Recognition, 1993. Proceedings CVPR '93., 1993 IEEE Computer Society Conference on*, pages 644–645, 1993.

[3] A. K. Jain, Lin Hong, S. Pankanti, and R. Bolle. An identity-authentication system using fingerprints. *Proceedings of the IEEE*, 85(9):1365–1388, 1997.

[4] Anil K. Jain and Kalle Karu. Learning texture discrimination masks. *IEEE Trans. Pattern Anal. Mach. Intell.*, 18(2):195–205, 1996.

[5] Anil K. Jain and David Maltoni. *Handbook of Fingerprint Recognition*. Springer-Verlag New York, Inc., Secaucus, NJ, USA, 2003.

[6] Xudong Jiang, M. Liu, and A. C. Kot. Reference point detection for fingerprint recognition. *Pattern Recognition, 2004. ICPR 2004. Proceedings of the 17th International Conference on*, 1:540–543 Vol.1, 2004.

[7] Erwin Kreyszig. *Advanced Engineering Mathematics*. Wiley, 6th edition, 1988.

[8] Jun Li, Wei-Yun Yau, and Han Wang. Constrained nonlinear models of fingerprint orientations with prediction. *Pattern Recognition*, 39(1):102–114, January 2006.

[9] D. Maio and D. Maltoni. A structural approach to fingerprint classification. *Pattern Recognition, 1996., Proceedings of the 13th International Conference on*, 3:578–585 vol.3, 1996.

[10] D. Maio, D. Maltoni, R. Cappelli, J. L. Wayman, and A. K. Jain. Fvc2000: fingerprint verification competition. *Pattern Analysis and Machine Intelligence, IEEE Transactions on*, 24(3):402–412, 2002.

[11] D. Maio, D. Maltoni, R. Cappelli, J. L. Wayman, and A. K. Jain. Fvc2002: Second fingerprint verification competition. *Pattern Recognition, 2002. Proceedings. 16th International Conference on*, 3:811–814 vol.3, 2002.

[12] Kenneth Nilsson and Josef Bigun. Localization of corresponding points in fingerprints by complex filtering. *Pattern Recogn. Lett.*, 24(13):2135–2144, September 2003.

[13] Sharath Pankanti, Salil Prabhakar, and Anil K. Jain. On the individuality of fingerprints. *IEEE Trans. Pattern Anal. Mach. Intell.*, 24(8):1010–1025, August 2002.

[14] A. R. Rao and R. Jain. Analyzing oriented textures through phase portraits. *Pattern Recognition, 1990. Proceedings., 10th International Conference on*, i:336–340 vol.1, 1990.

[15] A. R. Rao and R. C. Jain. Computerized flow field analysis: oriented texture fields. *Pattern Analysis and Machine Intelligence, IEEE Transactions on*, 14(7):693–709, 1992.

[16] A. R. Rao and B. G. Schunck. Computing oriented texture fields. *Computer Vision and Pattern Recognition, 1989. Proceedings CVPR '89., IEEE Computer Society Conference on*, pages 61–68, 1989.

[17] C. F. Shu, R. Jain, and F. Quek. A linear algorithm for computing the phase portraits of oriented textures. *Computer Vision and Pattern Recognition, 1991. Proceedings CVPR '91., IEEE Computer Society Conference on*, pages 352–357, 1991.

[18] Chiao-Fe Shu and Ramesh C. Jain. Direct estimation and error analysis for oriented patterns. *CVGIP: Image Underst.*, 58(3):383–398, November 1993.

[19] C. F. Shu and R. C. Jain. Vector field analysis for oriented patterns. *IEEE Trans. Pattern Anal. Mach. Intell.*, 16(9):946–950, September 1994.

[20] Shen Wei, Chen Xia, and Jun Shen. Robust detection of singular points for fingerprint recognition. *Signal Processing and Its Applications, 2003. Proceedings. Seventh International Symposium on*, 2:439–442 vol.2, 2003.

[21] Wei-Yun Yau, Jun Li, and Han Wang. Nonlinear phase portrait modeling of fingerprint orientation. *Control, Automation, Robotics and Vision Conference, 2004. ICARCV 2004 8th*, 2:1262–1267 Vol. 2, 2004.